MOX–Report No. 05/2011

An algorithm for the study of parameter dependence for hyperbolic systems

GIANNI ARIOLI MONICA GAMBA

An algorithm for the study of parameter dependence for hyperbolic systems

Gianni Arioli   Monica Gamba

MOX– Modellistica e Calcolo Scientifico
Dipartimento di Matematica "F. Brioschi"
Politecnico di Milano
via Bonardi 9, 20133 Milano, Italy
gianni.arioli@polimi.it, monica.gamba@polimi.it

Abstract

We introduce a new technique for computing the explicit dependence of the result of the numerical integration of a conservation law with respect to one or more parameters. The method is intrusive, but it relies on an automatic differentiation algorithm, therefore it requires minimal modifications of the code used for the plain numerical integration. We present an example of application to the study of the shock tube, that is Euler's system of equations with discontinuous initial conditions.

1   Introduction and motivations

Most mathematical models need to be complemented with data and parameters. These data may concern the geometry, the boundary and initial conditions, the external forces. The parameters may also describe the constitutive laws of the system. In many situations, the data and parameters cannot be exactly specified, because of some limitations in the experimental data available (for instance in the measurement or identification of some model constant), in the knowledge of the system (for instance in the early design stage, where the forcing and boundary conditions may not be precisely defined yet), or because of some inherent variability of the systems studied (for instance due to dimensional tolerances in the production and assembly process, variability in operating conditions, etc...). So, it is essential that an algorithm is robust with respect to a variation of the

parameters and data. Furthermore, it may be very useful to know the functional dependence of the results with respect of the parameters and data, in order to better understand and exploit the model. In fact, such knowledge can be very useful to tune the model, to characterize the robustness and controllability of the system, to perform risk analysis and to manage variability.

There is a vast literature on intrusive methods for uncertainty quantification, we refer e.g. to [A, LMK, TLMNE] and references therein. Those methods are focussed on the computation of the probability distribution of the output of the computation, given a probability distribution of the parameters in input. The general idea of those methods stems from the polynomial chaos introduced by Wiener [W]. The other basic fact about these methods is that the equations under study are projected on a suitable basis for the probability space, and such projection is then integrated.

Here we present a new approach to the problem of studying systems depending on parameters and data, and specifically of computing the functional dependence of the response of the system with respect to the parameters. Unlike the methods for uncertainty quantification and propagation, this technique is not focussed on the computation of the probability distribution of the response of the system, but on the determination of the functional dependence of the output with respect to the parameters. The method is intrusive and it relies on automatic differentiation algorithms.

The basic idea comes from the Taylor Models (TM) developed by Berz and Makino [BM1, BM2, BM3, BM4] to study dynamical systems whose initial data are intervals. Such idea, in turn, is a development of techniques of automatic differentiation. The key-word here is "automatic": this technique does not require new algorithms, nor significant changes in the equations describing the model; rather, by making extensive use of object oriented programming, it only requires a minor adaptation of the algorithms used to integrate the model with fixed values of the parameters. We focus the attention on computing the functional dependence of the result of the numerical integration of a nonlinear hyperbolic system with one parameter. Since hyperbolic systems can generate discontinuities such as shocks and contact waves, they could be a very good test. We choose as an example of a non linear hyperbolic system a well known system of conservation laws of the gas dynamics, the one dimensional Euler's equations, more precisely the shock tube introduced in [S].

In Section 2 we describe the general framework. In Section 3 we describe the experiment. In Section 4 we describe the results with the plain Taylor expansion. In Section 5 we analyze the shortcomings of the Taylor expansion and provide a correction.

2 Functional treatment of parameters

Consider a generic mathematical model depending on a parameter $x \in \mathbb{R}^N$ which we write in implicit form

$$F(y, x) = 0 \, . \tag{1}$$

We assume here that all data, e.g. initial or boundary values in the case where the model is a differential equation, are included either in the definition of F, or in some components of the parameter x. For generality, assume that the unknown y lies in a Banach space X, which will eventually be discretized. Assume that the parameter x ranges in some multiinterval, say $x \in X_0 = [x_1^a, x_1^b] \times \cdots \times [x_N^a, x_N^b]$. Our main aim is to find the explicit dependence on x of the solution y.

We present the method in the case $N = 1$, the extension to the general case being straightforward. The basic idea is to compute the Taylor expansion with respect to the parameter x of the solution. More precisely, we choose a degree K and define

$$y(x) = \sum_{k=0}^{K} y_k (x - x_0)^k \, . \tag{2}$$

The aim is to be able to compute the Taylor coefficients $\{y_k\}$ in the case when the direct computation of the derivatives of the function F is not available or it is not feasible, which is what happens in any non elementary computation. What we have in mind in this paper is the case where y represents the solution of a hyperbolic partial differential system solved by a simple numerical algorithm, but the method is quite general and applicable to a large variety of problems.

Recently, a similar approach has been used in the setting of computer assisted proofs, see e.g. [AK1, AK2, AK3, ADBB, ADBM] and references there. We refer to such papers for an extensive discussion of the main ideas, while, for the convenience of the reader, we describe here the basics.

It is straightforward to implement on a computer an arithmetic of Taylor polynomials. More precisely, one represents a Taylor polynomial as the list of the coefficients, and then implements a procedure that, given a scalar α and two Taylor polynomials T_1, T_2 (that is, their coefficients), computes the (coefficients of the) Taylor polynomial corresponding to $\alpha(T_1 * T_2)$, where $*$ is either the addition or the multiplication. This implies that, given a polynomial $p(x)$, it is possible to compute a Taylor polynomial $p(T_1)$, and since all analytic functions $f(x)$ can be approximated with polynomials, it is also possible to compute the Taylor approximation of $f(T_1)$. Using object-oriented programming and operator overloading, it is possible to define an "object Taylor" and a set of functions which perform the basic operations and the computation of the elementary functions. Then, the object Taylor can be treated as a floating point number, and most numerical algorithms can be implemented directly on such object, see Section 2.1 below, while some other algorithm may need some minor adaptation.

While the direct computation of the expansion (4) is feasible, it turns out that, in order to evaluate the effectiveness of the method, it is more convenient

to rescale the parameter to the interval $[-1, 1]$ by setting

$$x = x(\xi) = \frac{x_a + x_b}{2} + \frac{x_a - x_b}{2}\xi \text{ with } \xi \in [-1, 1] \tag{3}$$

and then looking for the expansion

$$y(\xi) = \sum_{k=0}^{K} c_k \xi^k. \tag{4}$$

In order to compute (4), all we have to do is solve (1) by our favorite numerical algorithm, using object Taylors instead of floating point numbers and setting the value of the parameter x as given in (3). We remark that the extension of the arithmetic of Taylor polynomials to the case where there are many variables is not trivial, but this problem has been addressed in [BM4], where a very efficient algorithm is presented.

As a very simple example of the technique, we show how to compute the eigenvalue of largest norm (and the corresponding eigenvector) of an $n \times n$ matrix $A(x)$ whose entries $\{A_{jk}(x)\}$ depend analitically on the parameter x.

2.1 A simple example

Let X the Banach algebra of functions analytic in the unit disk $D = \{z \in \mathbb{C} : |z| \le 1\}$ and such that, if

$$f(z) = \sum_{l=0}^{+\infty} f_l z^l,$$

then

$$\|f\| = \sum_{l=0}^{+\infty} |f_l| < +\infty.$$

For $j, k = 1, \ldots, n$, let $A_{jk}(z) \in X$ and

$$A_{jk}(z) = \sum_{l=0}^{+\infty} A_{jkl} z^l.$$

Given $w_0 \in X^n$, define recursively

$$\begin{array}{rcl} u_k & = & Aw_{k-1} \\ w_k & = & u_k/\|u_k\| \\ \mu_k & = & (w_k, Aw_k), \end{array} \tag{5}$$

where $(a, b) = \sum_j a_j \bar{b}_j$ and $\|a\|^2 = (a, a)$ for all $a, b \in X^n$. The following theorem can be proved by adapting standard methods of numerical analysis:

Theorem 2.1 *Assume that the matrix $A(z)$, whose entries are the functions $\{A_{jk}(z)\}$, admits n eigenpairs $\{\lambda_i(z), e_i(z)\}$ for all $z \in D$, and assume that $\lambda_i \in X$ and $\{e_i\}_l \in X$. Then $\mu_k \to \lambda_1$ in X and $w_k \to e_1$ in X^N, where μ_k w_k are as in (5).*

This result can be applied in a straightforward way to build a numerical algorithm that produces the Taylor expansion of any chosen order n of the largest eigenvalue of the matrix $A(z)$ and the corresponding eigenvector; it suffices to:

1. Compute the Taylor polynomial of degree n of each entry of the matrix:
   $A_{jk}(x) = \sum_{l=0}^{n} a_{jk}^l x^l$.

2. Define $w_0(x)$ as an arbitrary and constant Taylor polynomial of degree n,
   $w_0(x) = w_0$.

3. Repeat the steps in (5), using the arithmetics of polynomials described above, until a chosen tolerance is met.

We tested this example with the matrix

$$A(x) = \begin{pmatrix} \sin(x) & 1 \\ 1 & 1 \end{pmatrix}$$

whose largest eigenvalue (and its Taylor expansion at $x = 0$) can be computed explicitly:

$$\lambda(x) = \frac{1}{2} \left(\sqrt{\sin^2(x) - 2\sin(x) + 5} + \sin(x) + 1 \right). \tag{6}$$

Let $\{\lambda_k\}$, $k = 0, \ldots, 10$ be the first coefficients of the McLaurin expansion of $\lambda(x)$ computed with the algorithm presented above and let $\{\mu_k\}$, $k = 0, \ldots, 10$ be the coefficients computed by differentiating (6) explicitely. It turns out that $\max_k |\lambda_k - \mu_k| < 10^{-16}$.

3   The Euler system of equations

We test the method on a hyperbolic system of conservation laws, more precisely the one dimensional Euler system of equations. The main difficulty is that solutions can exhibit discontinuities due to development of shock and contact waves. Our purpose is estimate the performance of the method on describing accurately not only the full dynamics of the system, but in particular the discontinuites.

We choose the *shock tube problem* introduced in [S] as a test: the physical setup is a tube filled with gas initially divided by a membrane into two sections. The gas has a higher density and pressure in one half of the tube, than in the other half, with zero velocity everywhere. At time $t = 0$ the membrane is removed and the gas is allowed to flow. The result is a net motion in the direction of lower pressure.

The structure of this flow involves three distinct waves. Across two of these waves there are discontinuities in some of the variables. A shock wave propagates into the region of lower pressure; across this wave the density and the pressure jump to lower values and all the variables are discontinuous. A contact discontinuity also moves towards the region of lower pressure, but at lower speed; here only the density is discontinuous. The third wave moves in the opposite direction and has a different structure: indeed all the variables are continuous and there is a smooth transition. This is the rarefaction wave and the density of the gas decreases as this wave passes through.

We consider a tube of length $L = 1$. At first, we discretize the space by dividing the domain in $N = 100$ cells and we choose a time step Δt corresponding to Courant number equal to 0.9. The equation is

$$U_t + F(U)_x = 0 \,,$$

in $(t, x) \in [0, T] \times [0, 1]$, where

$$U = \begin{pmatrix} \rho \\ \rho v \\ \rho e \end{pmatrix} \quad \text{and} \quad F(U) = \begin{pmatrix} U_2 \\ \frac{U_2^2}{U_1} + p \\ (U_3 + p)\frac{U_2}{U_1} \end{pmatrix} \,.$$

We choose $T = 0.15$, since the waves which characterize the solution have time to fully develop, without reaching the boundaries of the tube. $\rho(t, x)$ is the density of the gas, $v(t, x)$ is the velocity, $e(t, x)$ is the energy density and $p(t, x)$ is the pressure. In order to have a closed set of equation, we need a relation between p, e, ρ, v, that is the equation of state of the gas. We choose the equation of state for a polytropic ideal gas, that is

$$e_i = \frac{p}{\rho(\gamma - 1)}$$

where $\gamma = c_p/c_v$ is the ratio of the specific heats at constant pressure and at constant volume and e_i is the internal energy density, defined by

$$e = e_i + \frac{1}{2}v^2 \,.$$

The initial conditions of the experiment are:

$$(\rho(0, x), v(0, x), p(0, x)) = \begin{cases} (1, 0, 1) & \text{if} \quad x \in [0, 1/2] \\ (1/8, 0, 1/10) & \text{if} \quad x \in (1/2, 1] \,. \end{cases}$$

Since the nodes close to the boundary are uneffected by the experiment, the boundary conditions are irrelevant, as long as they do not introduce any kind of new dynamics. We use absorbing boundary conditions, implemented by adding one ghost cell at each end of the tube, and using a zeroth order extrapolation to assign values to them.
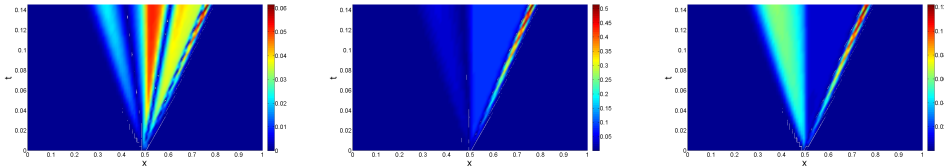
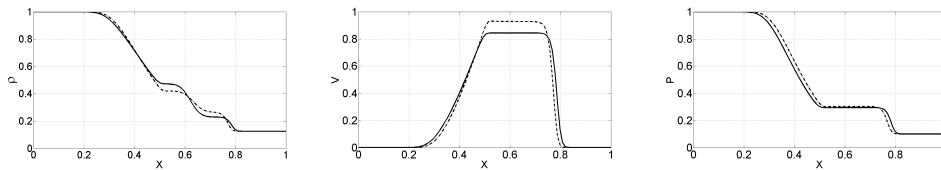Figure 1: Picture in space and time of the differences of ρ, v and p

Figure 2: Picture at time $t = T$ of ρ, v and p at the extreme values of γ

The variable parameter is γ. Since monoatomic gases have $\gamma = 5/3$ and biatomic gases have $\gamma = 7/5$, we consider γ varying in the interval $[7/5, 5/3]$. The shock wave travels to the right at speed $v + c(\gamma)$, where the speed of sound $c(\gamma)$ is given by $c(\gamma) = \sqrt{\gamma p/\rho}$, the rarefaction wave travels to the left at speed $v - c(\gamma)$ and the contact discontinuity travels to the right at speed v. So, when γ takes values in an interval, the velocities of the shock and rarefaction waves also take values in an interval.

We compute a solution of the system with Roe's approximate Riemann solver. We refer to [R] for a description of the well known numerical algorithm: here we only point out that we implemented it "as is", except for the fact that we used "objects Taylor" instead of floating point numbers.

4 Taylor expansion

We integrate the equation from the initial condition at $t = 0$ until $t = T$. Figure 1 displays the difference of density, speed and pressure computed between the extreme values of γ for all $t \in [0, T]$, while Figure 2 displays the final values $(t = T)$ of the same variables. Here ρ, v and p have been computed by evaluating a fifth order Taylor expansion.

Figures 1 and 2 show clearly that the influence of the parameter γ is particularly relevant near the shock wave. In order to study the accuracy of the results, we define the estimated local error on a variable w as

$$\epsilon(x,t) := \left(\frac{1}{M} \sum_{i=0}^{M-1} \left(w^T(x,t,\xi^i) - w^N(x,t,\xi^i) \right)^2 \right)^{1/2} \tag{7}$$

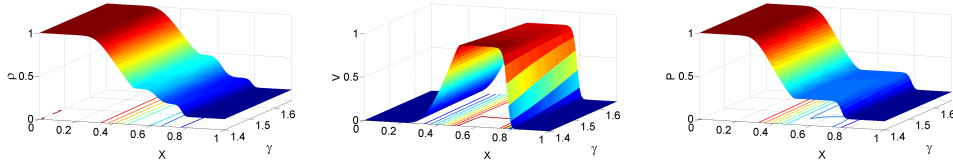where $w^T(x,t,\xi)$ e $w^N(x,t,\xi)$ are computed for a specific value of ξ (the rescaled

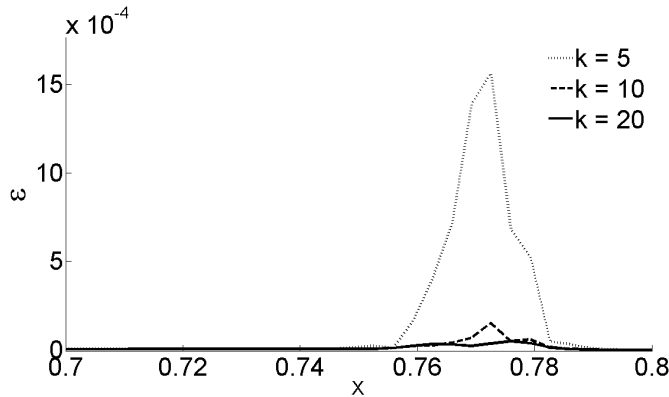Figure 3: Picture at time $t = T$ of ρ, v and p for all values of γ

Figure 4: Error on the density at different Taylor orders

parameter, see (3)) respectively by evaluating the Taylor expansion and by solving directly the numeric problem. We set $\xi^i = -1 + 2i/(M-1)$.

Figure 4 displays the estimated errors on the density at different Taylor orders. It is quite clear that, by using a sufficiently high order, it is possible to obtain very accurate results.

5   A finer grid

The results obtained in Section 4 show that it is possible to represent the solution of the Euler system with a very good precision on a grid of 100 points. In order to test the efficacy of the method to represent discontinuities, we increase the spatial resolution, that is we use a finer grid. The experiments show that it is possible to do so only up to a point: when the partition exceeds $N = 300$ the errors in the region close to the shock wave become larger and larger. Figure 5 on the left shows ρ for different values of the parameter in the region close to the shock wave: note that, while the result is realistic for values of the parameter close to the center of the interval, this is not the case when the parameter takes the largest and the smallest value. The picture on the right shows ρ with $\gamma = 1.4$, with the computation performed at different orders. We observe that the oscillations become wider with a larger order. Figure 6 on the left shows the estimated error on ρ, with the full interval for the parameter γ. Figure 6 on the right shows the
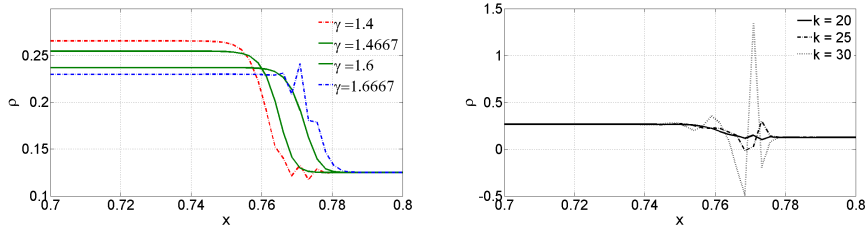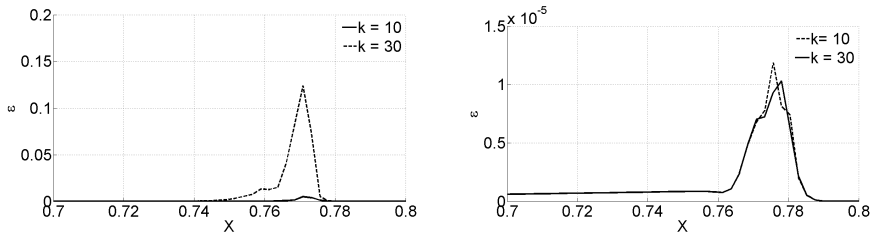
Figure 5: Density with $N = 400$

Figure 6: Error on the density with $\gamma \in [1.4, 1.67]$ and $\gamma \in [1.47, 1.6]$.

same error, but with the interval of variability of γ cut in half. The fact that the errors are a few order of magnitude larger, when a wider interval is considered, and that an increase of the order of the expansion does not improve the accuracy hints to the fact that the Taylor expansion fails. A similar phenomenon occurs for the other physical variables. A possible explanation of this behavior is that the radii of convergence of the Taylor series in the rescaled variable ξ, representing the physical variables in the nodes close to the shock become smaller than 1. So, it appears useful to attempt to estimate the radius of convergence of the Taylor expansion. In order to do that, we compute the coefficients of a geometric series

$$S^* = \sum_k \frac{Ax^k}{(r^*)^k} \tag{8}$$

which is the best approximation (in the sense of the least squares) of the Taylor polynomial

$$S = \sum_k C_k x^k \,, \tag{9}$$

that is, we compute A and r^* which best fit the equality

$$|C_k| = \frac{A}{(r^*)^k} \,.$$

Figure 7 shows the estimated radius of convergence of the Taylor expansion of order 30 for the density, in the region around the shock, for different values of the partition of the grid. We observe that the radius decreases below the value 1 when $N > 300$.
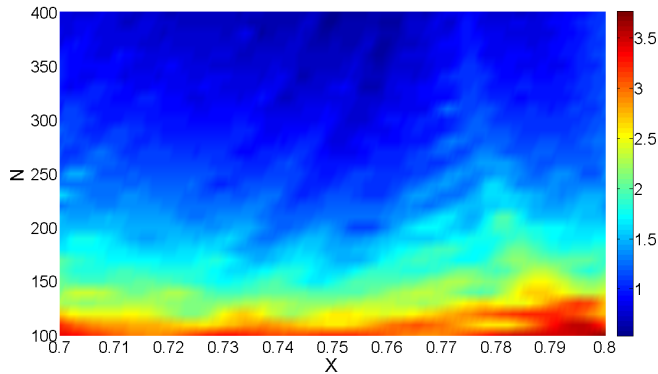
9

Figure 7: Estimate of the radius of convergence in the region close to the shock
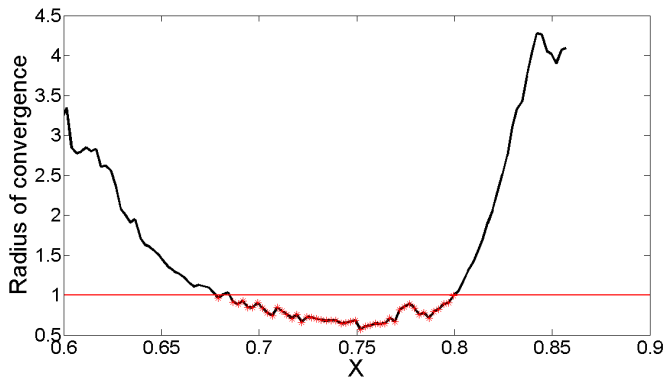

Figure 8: Radii of convergence

It turns out that, in order to have a better description of the shock wave, it is necessary to use a finer grid and, at the same time, to decrease the width of the interval where the parameter ranges. In order to cover the entire original interval, it would be necessary to partition it in subintervals and repeat the computation for each subinterval. For example, in order to be able to use $N = 400$, it is necessary to decrease the width of the interval to roughly 30% of the original value. Figure 8 displays the estimated radii of convergence of the Taylor expansion of the density in the region close to the shock wave, with $N = 400$. In the next Section we develop a method to address this issue.

6   A deformation of the domain of the parameter

The experiments of the previous section have shown some evidence that the Taylor expansion of the physical variables has singularities in the complex plane, which move closer to the real axis (and therefore inside the circle of radius one

centered at the point where the expansion is computed), when the grid is made finer. Therefore, the functions describing the variables of the equations with respect to the parameter do not seem to be analytic in the whole circle and, in order to study the system when the parameter varies in the original interval, we would be forced to partition it in smaller subintervals and repeat the whole computation once for each subinterval.

This approach has a clear disadvantage: not only it forces us to integrate the system as many times as the number of subintervals, but also it does not provide us with a single polynomial expansion of the dependence of the result with respect to the parameter. Since the region of convergence appears to be bounded by singularities close to the real axis, we may try to find a holomorphic map that deforms it into a circle. Using this map, we can substitute the circle of convergence with a region of analyticity closer to the real axis. This can be done e.g. by the change of variable described below.

Let $D \subset \mathbb{C}$ be defined by $D = \{z \in \mathbb{C} : |z| \leq 1\}$. Fix $p > 0$ and consider the map $\varphi_p : D \to \mathbb{C}$ defined by

$$\varphi_p(z) = \frac{(1+z)^p - (1-z)^p}{(1+z)^p + (1-z)^p}.$$

The map is holomorphic, injective and $\varphi_p([-1,1]) = [-1,1]$. Let $E_p = \varphi_p(D)$; then $\varphi_p^{-1} : E_p \to D$ is defined simply by $\varphi_p^{-1} = \varphi_{1/p}$. The blue curves in Figure 9 represent the images through the map $\varphi_{1/4}$ of the circles of radii $0.1k$, $k = 1 \ldots, 10$. If $p < 1$, $E_p \subset D$ and a circle is mapped into a curve compressed in the imaginary direction. Now we return to the original problem, where we have a function $f : D \to \mathbb{C}$ which is holomorphic, except for a singularity in $z_0 \in D$, $|z_0| < 1$. Clearly, there could be more singularities: what really matters is that the function is holomorphic in E_p, for some value of p; in other words, the singularities should not come too close to the real axis. We wish to expand f in power series centered in 0. If we fix some $p < 1$ such that no singularities are in E_p, then we can consider a change of variables $w = \varphi_p(z)$ so that for all $z \in D$ we have $w \in E_p$. Therefore the function defined by $g(z) = f(\varphi_p(z))$ is holomorphic in D, there exist coefficients c_k such that

$$g(z) = \sum_k c_k z^k$$

and the radius of convergence is 1.

6.1 Results on Euler System

We choose $p = 1/4$: a smaller value would reduce even further the region of analyticity, but it would also require a higher order, because, as it is evident from Figure 9, the map introduces a large distorsion close to the points 1 and -1. We apply the change of variables to the rescaled parameter, obtaining $w = \varphi_p(\xi)$ varying in E_p instead of ξ varying in D.
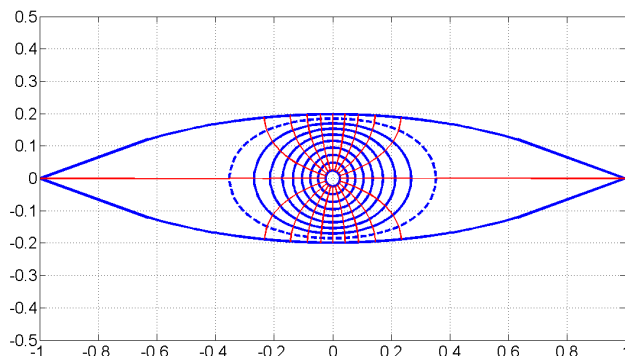
Figure 9: Image of $E_{1/4}$

In order to avoid the distorsion of the map near the extreme values $\{-1, 1\}$, we rescale the parameter in such a way that the maximum and minimum value of γ are assumed at $\xi = \pm 0.9$. The circle of radius $r = 0.9$ is mapped through $\varphi_{1/4}(\xi)$ to the dashed curve in Figure 9. The variability on γ is now defined by:

$$\gamma(\xi) = \frac{23}{15} + \frac{2/15}{\varphi_{1/4}(0.9)} \varphi_{1/4}(\xi), \qquad \xi \in [-0.9, 0.9]. \tag{10}$$

In order to integrate the system with the variability on γ defined by (10), we only have to substitute the explicit expression of the map $\varphi_{1/4}(\xi)$ in (10) with its power series expansion:

$$\gamma(\xi) = \frac{23}{15} + \frac{2/15}{\varphi_{1/4}(0.9)} \sum_k c_k \xi^k, \qquad \xi \in [-0.9, 0.9].$$

Now we can use the algorithm described in the previous sections without any further changes.

In Figure 10 we compare the error on the density obtained with the expansion with the holomorphic change of variable (dashed line) with the error obtained with the plain Taylor expansion (continuous line), at $N = 400$ and expansion order $k = 30$. The advantage of the use of the holomorphic deformation of the domain of the parameter is evident.

Figure 11 shows the density evaluated by the series expansion of order 30 at $\xi = -0.9$ and time $t = T$, for different values N of the spatial discretization. We observe the expected increase of sharpness with finer grids.

Figure 12 displays the estimated error on the density with $N = 600$. As we can see, we can increase the spatial resolution up to $N = 600$, maintaining the error within a magnitude 10^{-4}, with an expansion of order 30. If we want to increase further the spatial resolution, e.g. $N = 700$, we get again oscillations close to the shock wave for the extreme values of ξ. This appears again to be
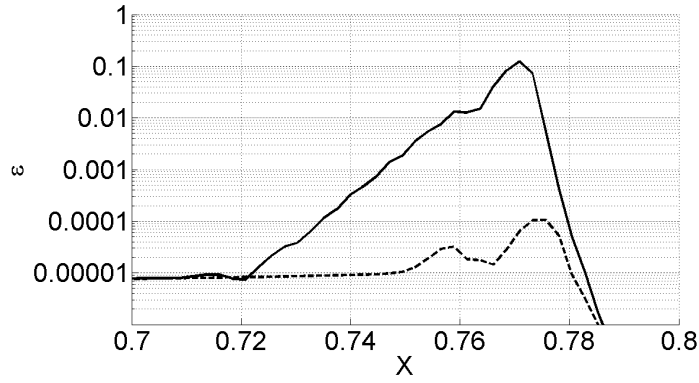
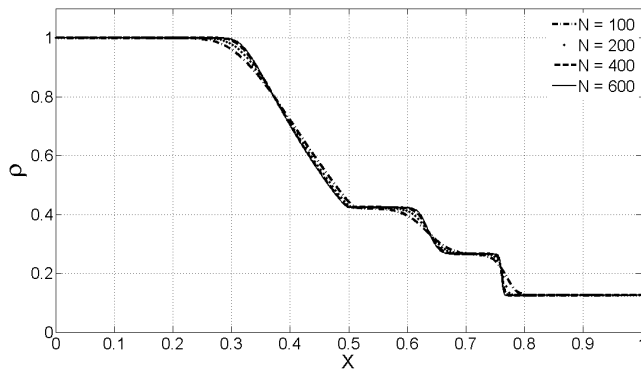Figure 10: Error on the density at $t = T$ with $N = 400$

Figure 11: Density at $t = T$ and $\xi = -0.9$

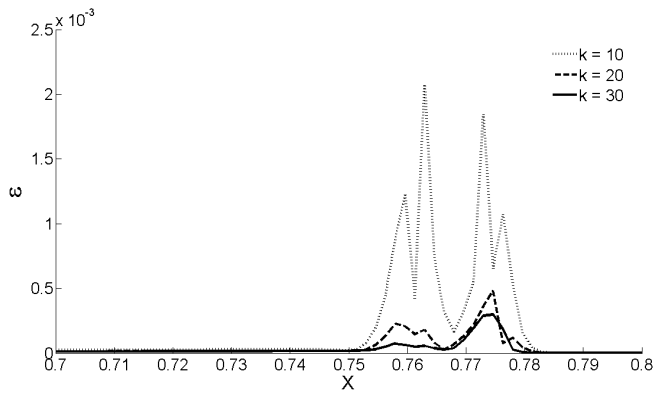Figure 12: Error on the density at $t = T$ and $N = 600$

motivated by the fact that some singularity approaches the real axis and enters $E_{1/4}$. We observe again that these oscillations cannot be reduced by increasing the order of the truncation of series.

7 Conclusions

The method introduced in this paper provides a very effective tool for studying the dependence of the dynamics of a hyperbolic system to a parameter (and it could be extended in a straightforward way to many parameters). Among the advantages, it does not require any major change of the numerical algorithms used to solve the system. Its main drawback is that, since it relies on a Taylor expansion, it loses applicability in presence of sharp discontinuities. By the change of variables introduced in Section 6 we can manage to partially overcome this problem and obtain reliable results even with a rather fine grid. In a forthcoming paper we will provide an alternative expansion, based on Chebyshev polynomials, which is much more effective to deal with a fine grid.

References

[A] R. Abgrall, *A simple, flexible and generic deterministic approach to uncertainty quantifications in non linear problems: application to fluid flow problems*, submitted to Journal of Computational Physics, also http://hal.inria.fr/index.php?halsid= fgtbktqaqhu7ht3042c6a137s4&view_this_doc=inria-00325315&version=1

[AK1] G. Arioli, H. Koch, The critical renormalization fixed point for commuting pairs of area-preserving maps, Comm. Math. Phys. 295 (2010) 415-429

[AK2] G. Arioli, H. Koch, Computer-assisted methods for the study of stationary solutions in dissipative systems, applied to the Kuramoto-Sivashinski equation, Arch. Rational Mech. An. 197 (2010) 1033

[AK3] G. Arioli, H. Koch, Integration of dissipative PDEs: a case study, SIAM J. of Appl. Dyn. Syst., 9 (2010) 1119-1133

[ADBM] Armellin, R.; Di Lizia, P.; Berz, M.; Makino, K. Computing the critical points of the distance function between two Keplerian orbits via rigorous global optimization. Celestial Mech. Dynam. Astronom. 107 (2010), no. 3, 377–395

[ADBB] Armellin, R.; Di Lizia, P.; Bernelli-Zazzera, F.; Berz, M. Asteroid close encounters characterization using differential algebra: the case of Apophis. Celestial Mech. Dynam. Astronom. 107 (2010), no. 4, 451–470

[BM1] K. Makino, M. Berz, *Higher order verified inclusions of multidimensional systems by Taylor models. Proceedings of the Third World Congress of Nonlinear Analysts, Part 5* (Catania, 2000). Nonlinear Anal. 47 (2001), no. 5, 3503–3514

[BM2] M. Berz, K. Makino, *Taylor models and other validated functional inclusion methods.* Int. J. Pure Appl. Math. 6 (2003), no. 3, 239–316

[BM3] M. Berz, K. Makino, *Taylor models and other validated functional inclusion methods.* Int. J. Pure Appl. Math. 4 (2003), no. 4, 379–456.

[BM4] M. Berz, K. Makino, *Higher Order Multivariate Automatic Differentiation, Validated Computation of Remainder Bounds*, Transactions on Mathematics 3(1) (2004) 37-44

[LMK] O.P. Le Maître and O.M. Knio, Spectral Methods for Uncertainty Quantification with Applications to Computational Fluid Dynamics

[R] P.L. Roe, *Approximate Riemann Solvers, Parameter Vectors, and Difference Schemes*, J. of Comp. Phys. 135, (1997) 250-258

[S] G.A. Sod, *A Survey of Several Finite Difference Methods for Systems of Nonlinear Hyoerbolic Conservation Laws*, J. Comp. Phys. 27 (1978) 1-31

[TLMNE] J. Tryoen, O. Le Maître, M. Ndjinga, A. Ern, *Roe solver with entropy corrector for uncertain hyperbolic systems*, Journal of Computational and Applied Mathematics 235 (2010) 491-506

[W] N. Wiener, *The homogeneous chaos*, American Journal of Mathematics Vol. 60, No. 4 (Oct., 1938), pp. 897-936

MOX Technical Reports, last issues

Dipartimento di Matematica "F. Brioschi",
Politecnico di Milano, Via Bonardi 9 - 20133 Milano (Italy)

05/2011   GIANNI ARIOLI, MONICA GAMBA:
An algorithm for the study of parameter dependence for hyperbolic systems

04/2011   FRANCESCA IEVA, ANNA MARIA PAGANONI,
DAVIDE PIGOLI, VALERIA VITELLI:
Multivariate functional clustering for the analysis of ECG curves morphology

03/2011   GIULIA GAREGNANI, GIORGIO ROSATTI, LUCA BONAVENTURA:
Mathematical and Numerical Modelling of Fully Coupled Mobile Bed Free Surface Flows

02/2011   TONI LASSILA, ALFIO QUARTERONI, GIANLUIGI ROZZA:
A reduced basis model with parametric coupling for fluid-structure interaction problems

01/2011   M. DALLA ROSA, LAURA M. SANGALLI, SIMONE VANTINI:
Dimensional Reduction of Functional Data by means of Principal Differential Analysis

43/2010   GIANCARLO PENNATI, GABRIELE DUBINI,
FRANCESCO MIGLIAVACCA, CHIARA CORSINI,
LUCA FORMAGGIA, ALFIO QUARTERONI,
ALESSANDRO VENEZIANI:
Multiscale Modelling with Application to Paediatric Cardiac Surgery

42/2010   STEFANO BARALDO, FRANCESCA IEVA,
ANNA MARIA PAGANONI, VALERIA VITELLI:
Generalized functional linear models for recurrent events: an application to re-admission processes in heart failure patients

41/2010   DAVIDE AMBROSI, GIANNI ARIOLI, FABIO NOBILE,
ALFIO QUARTERONI:
Electromechanical coupling in cardiac dynamics: the active strain approach